Direct-numerical-simulation-based measurement of the mean impulse response of homogeneous isotropic turbulence

Marco Carini[*] and Maurizio Quadrio[†]

Dipartimento di Ingegneria Aerospaziale, Politecnico di Milano, Campus Bovisa, Via La Masa 34, 20156 Milano, Italy
(Received 4 May 2010; revised manuscript received 6 October 2010; published 1 December 2010)

A technique for measuring the mean impulse response function of stationary homogeneous isotropic turbulence is proposed. Such a measurement is carried out here on the basis of direct numerical simulation (DNS). A zero-mean white-noise volume forcing is used to probe the turbulent flow, and the response function is obtained by accumulating the space-time correlation between the white forcing and the velocity field. This technique to measure the turbulent response in a DNS numerical experiment is a research tool in that field of spectral closures where the linear-response concept is invoked either by resorting to renormalized perturbations theories or by introducing the well-known fluctuation-dissipation relation (FDR). Although the results obtained in the present work are limited to relatively low values of the Reynolds number, a preliminary analysis is possible. Both the characteristic form and the time scaling properties of the response function are investigated in the universal subrange of dissipative wave numbers; a comparison with the response approximation given by the FDR is proposed through the independent DNS measurement of the correlation function. Very good agreement is found between the measured response and Kraichnan's description of random energy-range advection effects.

I. INTRODUCTION

The concept of impulse response tensor of an isotropic turbulent flow lies at the heart of the direct interaction approximation (DIA) theory, developed 50 years ago [1] by the great theoretical physicist Kraichnan, to tackle the turbulence closure problem analytically. Since then, within the renormalized perturbations approach, several closure strategies have been proposed (a significant example is the local energy transfer (LET) theory introduced by McComb [2]), eventually adopting a Lagrangian viewpoint, as done by Kraichnan himself [3,4] and others [5,6]. In all such theories, either Eulerian or Lagrangian, closure is achieved by means of a closed set of integro-differential equations, where the unknowns are the two-point two-time velocity correlation tensor and the response tensor itself. An exception is LET, where the response tensor is replaced with a renormalized propagator tensor which connects the velocity correlations at different times, in close analogy with the well-known fluctuation-dissipation relation of the classical statistical physics. Recently, Kiyani and McComb [7] showed how a renormalized response tensor relating the two-point covariance at different times can be derived; the corresponding relationship reduces to a fluctuation-dissipation relation (FDR) form, still within the theoretical framework of second-order renormalized perturbations, by introducing the so-called time ordering approach to reconcile the time symmetry of the correlation with the causality of the response.

During the last decades, several statistics of homogeneous isotropic turbulence (HIT), either computed with well-resolved direct numerical simulations or obtained from experiments, have been compared to the corresponding theoretical predictions at increasing values of Re_λ [8], in the statistically stationary as well as in the freely decaying regime. Encouraging results both for the LET theory and various Lagrangian closures have been reported [6,9–11]. Up to the present day, however, such a comparison for the impulse response function has never been addressed, owing to the lack of (experimental or numerical) information about it. Missing such a comparison is not a minor issue for Eulerian closure theories: as stressed in Ref. [9], the differences among the various theoretical approaches have their roots in the form of the response or propagator equation, whereas the covariance equation is most often treated in equivalent ways. Furthermore, if the response and the two-point covariance were available, the degree of approximation involved in using the FDR in the context of HIT could be straightforwardly evaluated, indirectly gathering information about the invariant probability distribution of the turbulent system [12].

In recent years Luchini *et al.* in Ref. [13] proposed an original method to carry out an Eulerian direct-numerical-simulation (DNS)-based measurement of the mean impulse response of a turbulent flow and described the response function of a fully developed turbulent channel flow to small-amplitude perturbations applied at the wall. That study was conceived in the framework of turbulence control (hence the emphasis on wall flows and wall forcing); due to lack of isotropy, the response tensor is quite complicated and does not directly relate to the previous isotropic theories. However, the proposed measurement technique provides us with the required tools to obtain the impulse response tensor for HIT, where the response function shall be intended to describe the response of turbulence to volume forcing. The present paper therefore aims at measuring the Eulerian HIT response, presenting preliminary results, obtained at low values of Re_λ, which will enable us to analyze the characteristic form and time scales of the response and to compare them with theoretical predictions and assumptions.

The paper is organized as follows. In Sec. II, the definition of the impulse response is briefly reviewed to introduce

*carini@aero.polimi.it
†maurizio.quadrio@polimi.it

the measurement technique, which is numerically validated against the available analytical viscous solution, and to discuss accuracy issues. In Sec. III the actual response function is presented and analyzed with reference to the theoretical background of renormalized perturbations and FDR. Lastly, Sec. IV is devoted to a concluding discussion.

II. MEASURING THE RESPONSE FUNCTION BY DNS

A. Definition of the impulse response function

Following Ref. [14], the most general definition in wave-vector space $\boldsymbol{\kappa}$ of the instantaneous impulse response tensor of a turbulent velocity field $\boldsymbol{u}(\boldsymbol{\kappa},t)$ to an external volume force $\boldsymbol{f}(\boldsymbol{\kappa},t)$ is given by the following input-output relationship between infinitesimal perturbations δ [note the different notation from the Dirac delta function $\delta(\cdot)$]:

$$\delta u_i(\boldsymbol{\kappa},t) = \int \int_{-\infty}^{t} H_{in}(\boldsymbol{\kappa},\boldsymbol{\kappa}',t,t')\delta f_n(\boldsymbol{\kappa}',t')dt'd\boldsymbol{\kappa}'. \quad (1)$$

It is important to underline that perturbations assume here a stochastic meaning since they are superimposed to a particular random realization of $\boldsymbol{u}$, which itself is a solution of the fully nonlinear Navier-Stokes equations (NSEs) in Fourier space. Therefore, $H_{in}(\boldsymbol{\kappa},\boldsymbol{\kappa}',t,t')$ possesses a random nature, and an integral formulation not only in time but also in wave-vector space is required. In fact the instantaneous response tensor plays the role of a tangent Green's function, related to a random and nonlinear state, and satisfies the instantaneous response equation

$$\left(\frac{\partial}{\partial t} + \nu\kappa^2\right)H_{in}(\boldsymbol{\kappa},\boldsymbol{\kappa}',t,t')$$

$$= 2M_{ijm}(\boldsymbol{\kappa})\int u_j(\boldsymbol{p},t)H_{mn}(\boldsymbol{\kappa}-\boldsymbol{p},\boldsymbol{\kappa}',t,t')d\boldsymbol{p}$$

$$+ P_{in}(\boldsymbol{\kappa}')\delta(\boldsymbol{\kappa}-\boldsymbol{\kappa}')\delta(t-t'), \quad (2)$$

which can be derived through a stochastic Green's-function formalism applied to the linearized form of Fourier-transformed NSEs. In Eq. (2) $M_{ijm}(\boldsymbol{\kappa})$ is the inertial transfer operator given by

$$M_{ijm}(\boldsymbol{\kappa}) = -i/2[\kappa_m P_{ij}(\boldsymbol{\kappa}) + \kappa_j P_{im}(\boldsymbol{\kappa})], \quad (3)$$

and $P_{ij}(\boldsymbol{\kappa})$ is the projection tensor in wave-vector space, expressed as

$$P_{ij}(\boldsymbol{\kappa}) = \delta_{ij} - \kappa^{-2}\kappa_i\kappa_j. \quad (4)$$

The locality of the response tensor in wave-vector space follows only after averaging:

$$\langle H_{in}\rangle = \mathcal{H}_{in}(\boldsymbol{\kappa},t,t')\delta(\boldsymbol{\kappa}-\boldsymbol{\kappa}'). \quad (5)$$

Lastly, exploiting statistical isotropy and stationarity results in scalar response functions, respectively, $\hat{\mathcal{G}}$ and $\mathcal{G}$, defined as follows:

$$\mathcal{H}_{in}(\boldsymbol{\kappa},t,t') = P_{in}(\boldsymbol{\kappa})\hat{\mathcal{G}}(\kappa,t,t'), \quad (6)$$

$$\mathcal{G}(\kappa,\tau) = \hat{\mathcal{G}}(\kappa,t,t-\tau). \quad (7)$$

The causality property holds for both the previous functions; hence,

$$\mathcal{G}(\kappa,\tau) = 0 \quad \text{for } \tau < 0, \quad \forall \kappa. \quad (8)$$

This is obviously a consequence of the realizability of the dynamical system that is being described through its impulse response. As indicated by Kraichnan [1], the scalar response is a real unit-bounded function,

$$|\mathcal{G}(\kappa,\tau)| \leq \mathcal{G}(\kappa,0^+) = 1, \quad \forall \tau > 0, \quad \forall \kappa. \quad (9)$$

B. Direct numerical simulation

The measurement of $\mathcal{G}$ described in this paper is carried out by means of a forced DNS of stationary HIT on a cubic domain, whose edge length L is chosen to be $L=2\pi$ for convenience, so that the fundamental wave number is $\kappa_0 = 2\pi/L = 1$ without loss of generality. A numerical code has been developed on purpose and equipped with parallel (shared-memory) computing capabilities. The code implements a classical Galerkin-Fourier scheme applied to the velocity-vorticity formulation of the incompressible Navier-Stokes equations. In the present context, this formulation presents interesting advantages in terms of memory requirements. Exact removal of the aliasing error is obtained with the 3/2 zero-padding rule; time integration is carried out by means of a third-order low-storage Runge-Kutta (Williamson) scheme; see Refs. [15,16] for additional numerical details. The forcing scheme has been carefully implemented following the provisions stated in Ref. [17], from which the notation adopted below is borrowed. The Kolmogorov scale is indicated with η, with $\kappa_d = \eta^{-1}$, the instantaneous dissipation rate is ε, the forcing-containing shell is κ_f, and the mean energy injection rate is P that equals $\langle \varepsilon \rangle$ at statistical stationarity. Then the adopted feedback-acceleration forcing [17] is formulated in wave-number space as follows:

$$\boldsymbol{f}(\boldsymbol{\kappa},t) = \frac{Ph(\boldsymbol{\kappa};\kappa_f)}{2k_f(t)}\boldsymbol{u}(\boldsymbol{\kappa},t), \quad (10)$$

where $k_f(t)$ represents the kinetic energy of the modes within the forced shell κ_f and $h(\boldsymbol{\kappa};\kappa_f)$ is the related indicator function:

$$h(\boldsymbol{\kappa};\kappa_f) = \begin{cases} 1, & |\boldsymbol{\kappa}| \leq \kappa_f \\ 0, & \text{otherwise}. \end{cases} \quad (11)$$

A standard resolution of $\kappa_{max}\eta = 1.5$ is adopted, where κ_{max} indicates the maximum resolved wave number in each direction of the Fourier space. The numerical code has been thoroughly verified by running conventional simulations of stationary HIT. The computed energy spectra at various Re_λ's compare very well to available results. A comparison of this kind is shown in Fig. 1, which shows excellent agreement between our computed energy spectra and those published in Ref. [17]. The spectral code has been run on a machine equipped with 4 Opteron 2378 processors, where a case with
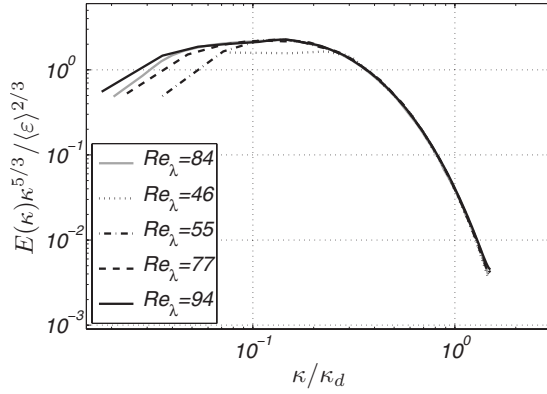
FIG. 1. Compensated energy spectrum for HIT: the function $E(\kappa)$ computed with the present DNS code at several values of Re_λ is compared with results from Ref. [17] at $\mathrm{Re}_\lambda = 84$.

$N = 256$ has a memory requirement of 940 Mbytes and a typical execution time of 11 s for one Runge-Kutta time step.

C. Response measurement technique

In Ref. [13] Luchini *et al.* proposed an innovative method for measuring the linear impulse response of a turbulent velocity field, resorting to the statistical statement of the input-output relation for a linear system, i.e., *the input-output correlation*. This approach is primarily motivated by the problem of low signal-to-noise ratio (S/N) that one would face, should the response function be measured according to its definition. Indeed the linear response of a nonlinear dynamical system is obtained by means of infinitesimal perturbations around an equilibrium state, which has a stochastic meaning in the description of turbulence. Therefore, impulsive perturbations externally introduced into the turbulent field to measure its linear response must be extremely small compared to the natural turbulent fluctuations for Eq. (1) to hold; as a consequence, their effect is buried into turbulent noise.

By definition the impulse response is the output of a linear system when either harmonic or impulsive signals are used as inputs. However, for a linearized turbulent system, the use of a proper statistical probe instead of a deterministic one will dramatically improve the computational efficiency of the overall measurement procedure. This is the case of using a white-noise process in input to the system. Indeed it is well known from filtering theory [18] that when a linear system is fed with white noise, the correlation between the input and the output is proportional to the impulse response of the system, owing to the delta-correlated property of the white-noise process. We employ an externally generated random volume forcing as the input; by computing its cross correlation with the velocity field, the whole wave-number dependency of the response function is obtained at once. At the same time, forcing is uniformly distributed over time and space, thus leading to improved S/N and larger allowed amplitudes within the linearity constraint. Therefore, this strategy performs much better than a deterministic forcing, be it either harmonic or impulsive, which would lead to computationally unaffordable simulations, as highlighted in Ref. [13].

Starting from Eq. (1), the input-output correlation can be written as

$$\langle \delta u_i(\boldsymbol{\kappa}, t) \delta f_j(-\boldsymbol{\kappa}, t-\tau) \rangle$$

$$= \int \int_{-\infty}^{+\infty} \mathcal{H}_{in}(\boldsymbol{\kappa}, t-t') \delta(\boldsymbol{\kappa}' - \boldsymbol{\kappa}) \langle \delta f_n(\boldsymbol{\kappa}', t')$$

$$\times \delta f_j(-\boldsymbol{\kappa}, t-\tau) \rangle dt' d\boldsymbol{\kappa}', \qquad (12)$$

where Eq. (5) has been used owing to the average operator, and the response causality property allows the extension toward $+\infty$ of the upper bound of time integral. Assuming $\delta f_j(\boldsymbol{\kappa}, t) = \epsilon w_j(\boldsymbol{\kappa}, t)$, with $\epsilon \in \mathbb{R}^+$ being a scale factor and $w_j(\boldsymbol{\kappa}, t)$ an independently generated zero-mean white-noise field with identity covariance matrix,

$$\langle \delta f_n(\boldsymbol{\kappa}, t') \delta f_j(-\boldsymbol{\kappa}, t-\tau) \rangle = \epsilon^2 \delta_{nj} \delta(t' - t + \tau), \qquad (13)$$

the cross correlation at the left-hand side of Eq. (12) will result in the properly scaled response tensor:

$$\langle \delta u_i(\boldsymbol{\kappa}, t) \delta f_j(-\boldsymbol{\kappa}, t-\tau) \rangle = \epsilon^2 \mathcal{H}_{ij}(\boldsymbol{\kappa}, \tau). \qquad (14)$$

We shall denote by $\tilde{\boldsymbol{u}}(\boldsymbol{\kappa}, t)$ the turbulent velocity field when volume forcing with white spectrum is applied. If the perturbation is small enough for linearity to hold, i.e., $\epsilon \ll 1$, it follows that

$$\tilde{\boldsymbol{u}}(\boldsymbol{\kappa}, t) = \boldsymbol{v}(\boldsymbol{\kappa}, t) + \delta \boldsymbol{u}(\boldsymbol{\kappa}, t), \qquad (15)$$

where $\boldsymbol{v}(\boldsymbol{\kappa}, t)$ indicates a different realization of the turbulent fluctuating field with respect to the original field $\boldsymbol{u}(\boldsymbol{\kappa}, t)$, as a consequence of nonlinearity and stochastic behavior of NSEs. Then computing the correlation between $\tilde{\boldsymbol{u}}$ and $\delta \boldsymbol{f}$ results in

$$\frac{\langle \tilde{u}_i(\boldsymbol{\kappa}, t) \delta f_j(-\boldsymbol{\kappa}, t-\tau) \rangle}{\epsilon^2} = \frac{1}{\epsilon^2} [\langle v_i(\boldsymbol{\kappa}, t) \delta f_j(-\boldsymbol{\kappa}, t-\tau) \rangle$$

$$+ \langle \delta u_i(\boldsymbol{\kappa}, t) \delta f_j(-\boldsymbol{\kappa}, t-\tau) \rangle]. \qquad (16)$$

Since the applied random perturbation on forcing is uncorrelated with turbulent fluctuations, the term $\langle v_i(\boldsymbol{\kappa}, t) \times \delta f_j(-\boldsymbol{\kappa}, t-\tau) \rangle$ will be averaged out in the previous equation, leading to

$$\frac{\langle \tilde{u}_i(\boldsymbol{\kappa}, t) \delta f_j(-\boldsymbol{\kappa}, t-\tau) \rangle}{\epsilon^2} = \mathcal{H}_{ij}(\boldsymbol{\kappa}, \tau), \qquad (17)$$

where the input-output correlation law [Eq. (12)] has been used to handle the nonvanishing term (second term) at the right-hand side of Eq. (16). In this way it is still possible to measure the turbulent response using the cross correlation between the white-noise input and the whole turbulent velocity field.

At this point it may be useful to note explicitly that no relation exists between the energy-driving forcing [Eq. (10)] and the white-noise forcing applied for the response measurement [Eq. (13)]. The former obviously represents a mere artificial, but unavoidable, mechanism to drive the flow and maintain statistical stationarity, via supply of energy at large scales. The white noise, on the other hand, is an external field

of volume force that enters the stationary turbulent system, which includes the energy-driving forcing. The jth component of the white-noise field, $w_j(\boldsymbol{\kappa},t)$, is defined as

$$w_j(\boldsymbol{\kappa},t) = \exp(i2\pi\phi), \qquad (18)$$

where ϕ is the output of a random number generator with a uniform probability distribution in the interval $[0,1]$ [19]. Hence, the white noise is independent of both the turbulent fluctuations and the energy-driving forcing applied to them through the feedback formula (10). A feedback forcing loop should be considered when looking at the linear response for wave numbers contained in the forced shell; but, as already discussed, these are not of physical interest.

In the HIT case Eq. (6) provides us a convenient way of accumulating just the simple scalar version of the response tensor by means of shell averaging over tensor trace:

$$\oint \mathcal{H}_{ii}(\boldsymbol{\kappa},\tau)dS(\kappa) = 8\pi\kappa^2\mathcal{G}(\kappa,\tau). \qquad (19)$$

When measuring $\mathcal{G}(\kappa,\tau)$, a proper spatial and temporal discretization must be adopted. While in a DNS the discretization in κ is easily derived from the Fourier representation of the velocity field (as for the energy spectrum $E(\kappa)$; see Ref. [17]), the definition of the τ step is less obvious. Both the time resolution of the white-noise delta correlation, $\Delta\tau_w$, i.e., the time interval between successive updates of the random numbers, and the averaging time T_{av}, i.e., the time interval over which statistics are computed, must be chosen such that $\mathcal{G}$ is properly described and at the same time the computational requirements of the numerical simulation are kept reasonable. If τ_{min} indicates the smallest time scale at which proper convergence of the response is sought, $\Delta\tau_w$ must be chosen so that $\Delta\tau_w \lesssim \tau_{min}$. Assuming uniform sampling of the response in N_c time instants separated by $\Delta\tau$, the time horizon available to represent the decay of the entire response must be greater than the whole response decay time τ_{max} at the lower wave number in the range of interest, i.e., $N_c\Delta\tau \geq \tau_{max}$. Proper convergence of the average response obviously requires $T_{av}/\tau_{max} \gg 1$. Indeed, while κ_d controls $\Delta\tau$ resolution and then Δt, i.e., the time integration step, the largest inertial wave number dictates N_c and T_{av}.

Given such contrasting requirements, characterizing the function $\mathcal{G}(\kappa,\tau)$ in the whole universal range of scales via a sole measurement is possible but computationally demanding. Hence, the entire function $\mathcal{G}(\kappa,\tau)$ can be measured through more than one uniform τ grid, so that the response is probed within several subranges of scales, leveraging their reduced extent. $\mathcal{G}(\kappa,\tau)$ is then measured in a wide range of scales via a limited number of DNS runs, each of which requires roughly the same computational effort. These simulations are independent and can be run simultaneously if the available computing power allows. However, for the results to obey the linearity constraint, the level of the introduced "noise energy," $\epsilon\Delta\tau_w$, must be kept constant across the different $\Delta\tau$ resolutions adopted at different scales. This means that a larger $\Delta\tau$ implies a reduced noise amplitude ϵ and a

longer averaging time. This is partially compensated by the larger time step size allowed by the time resolution of the response at lower wave numbers.

D. Test case: The purely viscous Stokes response

The Stokes or viscous response represents the zero-order term in the expansion series of $\mathcal{G}$ as introduced in the context of renormalized perturbations (see Refs. [9,20]). The Stokes response $\mathcal{G}^{(0)}$ can be easily derived from Eq. (2) after the removal of nonlinear terms, thus providing the solution for pure viscous dynamics of the velocity field. Its analytical form reads

$$\mathcal{G}^{(0)}(\kappa,\tau) = \exp(-\nu\kappa^2\tau). \qquad (20)$$

It is important to notice that the Stokes response has a deterministic nature, owing to the linearity of the Stokes operator: Kraichnan usually refers to it as "statistically sharp." The exact Stokes solution provides a useful tool for the validation of the full measurement procedure. To this purpose, the Stokes response can be retrieved from a DNS of the fully nonlinear NSE through a numerical linearization. In this way the algorithm employed for the measurement in the turbulent case is exactly that previously described in Sec. II C, but a null initial condition is adopted, the energy-driving forcing of Eq. (10) is turned off, and only the white-noise perturbation is applied. If $\epsilon \ll 1$, no evolution toward turbulence dynamics is produced, and nonlinear terms $\mathcal{O}(\epsilon^2)$ can be neglected with respect to the linear ones $\mathcal{O}(\epsilon)$ defining the Stokes equation.

The Stokes response has been measured in numerical experiments with a spatial resolution of 32^3 modes (before dealiasing) and $N_c = 50$. In these simulations $\Delta\tau = \Delta\tau_w$ is adopted, and several values of $\Delta\tau_w$ are used to investigate time resolution effects. In Fig. 2 (top and center) the time decay of the Stokes response at $\kappa/\kappa_0 = 8$ is plotted. The exact solution and the measured one agree very well (top figure). At small viscous time separations, $\tau\nu\kappa^2 < 1$, proper convergence of the measured response toward the exact one is observed (center figure) to depend on the $\Delta\tau_w$ resolution. Convergence of the response for different noise amplitudes ϵ and averaging times T_{av} has been additionally verified (not shown). Lastly, the measured Stokes response plotted at different wave numbers (bottom figure) is observed to possess the expected collapse when local viscous time scaling is adopted for τ.

III. TURBULENT RESPONSE

Several DNSs have been run to measure the impulse response of homogeneous isotropic turbulence. They are grouped into simulations with 128^3, 192^3, and 256^3 Fourier modes before dealiasing. Table I summarizes the discretization parameters of the simulations carried out without white-noise forcing, whereas Table II lists all the simulation runs to measure the response function, together with the values of the parameters used to discretize and measure $\mathcal{G}(\kappa,\tau)$. The attained values of Re_λ are low or moderate, ranging from $Re_\lambda = 55$ to $Re_\lambda = 94$. Moreover, given our limited computa-
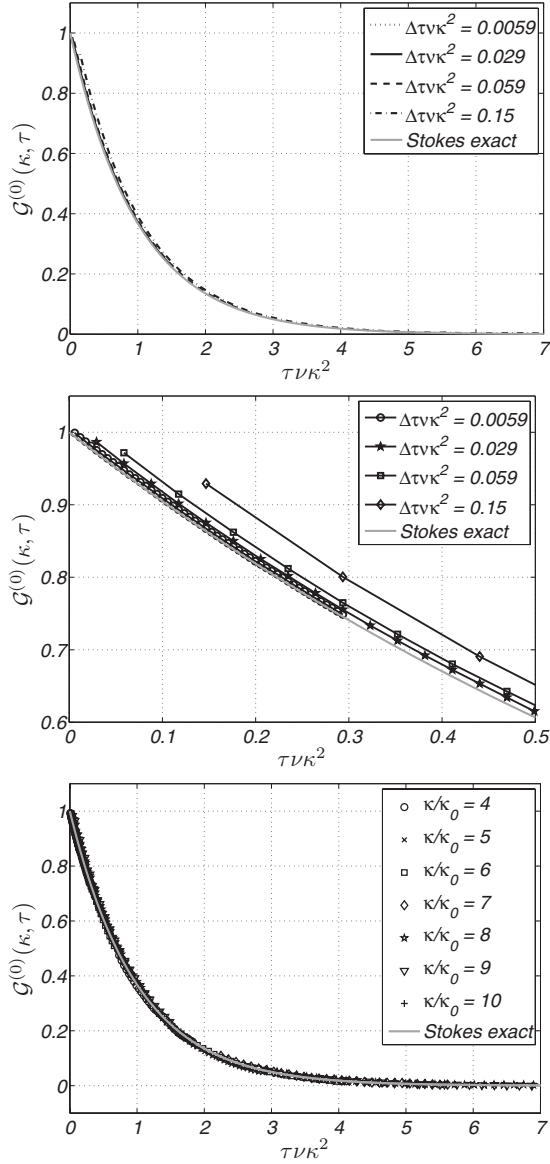
FIG. 2. Time decay of the measured Stokes response $\mathcal{G}^{(0)}$ at different $\Delta\tau$'s with $\epsilon=0.001$ and $T_{av}\nu\kappa^2=733.76$. Top: comparison between the measured and exact $\mathcal{G}^{(0)}$ at fixed $\kappa/\kappa_0=8$. Center: zoom of top plot for $\tau\nu\kappa^2 \ll 1$. Bottom: Stokes response at several wave numbers κ/κ_0 vs nondimensional time separation, emphasizing collapse with local viscous time scaling $\tau\nu\kappa^2$.

tional resources, the response is probed only at high wave numbers. As explained in Sec. II C, long averaging times are in fact required for proper convergence of the mean response at low wave numbers. However, it is important to emphasize

TABLE I. Parameters for the DNS of HIT carried out in the present work.

N	κ_{max}/κ_0	κ_d/κ_0	P	κ_f/κ_0	Re=$(\kappa_d/\kappa_f)^{4/3}$	Re$_\lambda$	$u_0(\kappa_f/P)^{1/3}$
128	42	28	1	3	20	55	1.7862
192	63	42	1	3	34	77	1.8453
256	84	56	1	3	49.5	94	1.8611

TABLE II. Discretization parameters for the DNS-based measurement of the response function.

N	Re$_\lambda$	Run	N_c	$\Delta\tau u_0\kappa_d$	ϵ	$T_{Av}u_0\kappa_d$
128	55	1	150	0.05202	0.00093	1.3004×10^5
		2	150	0.0322	0.0015	5643.7
192	77	1	150	0.0484	6.667×10^{-4}	9680
		2	150	0.0322	0.001	5643.7
256	94	1	150	0.0614	4.3529×10^{-4}	9981.6
		2	150	0.0376	7.1154×10^{-4}	6580
		3	150	0.0267	0.001	2069.2

here that the proposed measurement technique is capable of measuring the impulse response at any scale, provided that adequate computational resources are available.

In Sec. III A the linear behavior and the convergence of time averages are demonstrated, whereas in Sec. III B the behavior of the response and its scaling within the dissipative universal subrange are investigated. The correlation function is also computed during the stationary reference HIT simulations, so that a comparison with the impulse response function in terms of the classical FDR will be given at least in the range of scales considered here.

A. Linearity and time average

A key issue when measuring the response function $\mathcal{G}(\kappa,\tau)$ is the proper choice of amplitude ϵ for the white-noise forcing. Indeed the true turbulent impulse response reduces to its linear counterpart $\mathcal{G}$ only for vanishing noise energy, i.e., when $\epsilon\Delta\tau_w\to0$. In a finite setting, a reasonable preliminary requirement is that the white-noise forcing does not affect turbulence statistics appreciably. Then, suitable convergence of the measured response to $\mathcal{G}$ is observed when the function $\mathcal{G}/\epsilon$ becomes independent on ϵ. Indeed, as discussed in Sec. II C, given a time resolution $\Delta\tau_w$, ϵ represents the linearity control parameter. Since the white-noise forcing is spatially distributed over all the scales, the linearity threshold is fixed by perturbation effects on smallest scale dynamics, i.e., the viscous scales: when looking for the response at lower wave numbers with larger $\Delta\tau=\Delta\tau_w$, ϵ must be reduced to preserve the linear response at higher wave numbers.

Figure 3 provides a comparison between the energy spectrum $E(\kappa)$ computed in standard HIT DNS and those from simulations forced with white noise at Re$_\lambda=94$. Analogous results (not shown here) holds for the other spatial resolutions listed in Table II. The value of ϵ, which should be maximized in order to increase S/N and hence to reduce the required averaging time, is chosen so that marginal effects on the spectrum are confined within the numerical wave numbers larger than the Kolmogorov scale, $\kappa>\kappa_d$. Moreover, Table III quantifies the little variations in statistics such as $\langle\varepsilon\rangle$ and $\langle k\rangle$ due to white-noise forcing: $\Delta\langle\varepsilon\rangle$ and $\Delta\langle k\rangle$ are less then 0.4% and 1.9%, respectively. $\Delta\langle\varepsilon\rangle$, which is computed with respect to the exact asymptotic value P, is of the same order of the variations of $\langle\varepsilon\rangle$ observed in different runs of standard HIT DNS. $\Delta\langle k\rangle$, which is computed against the
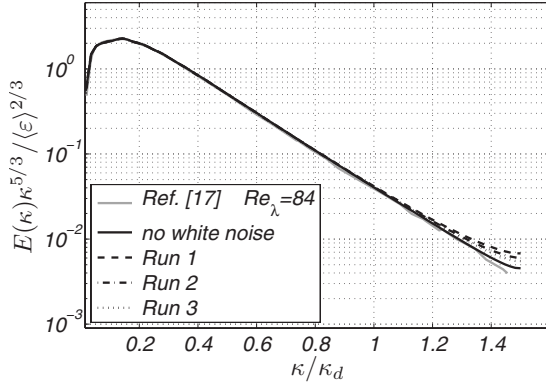
FIG. 3. Comparison between compensated energy spectra from HIT and from white-noise-forced HIT employed for measuring $\mathcal{G}(\kappa, \tau)$; $Re_\lambda = 94$ ($N = 256$) (cf. Table II). Note the absence of white-noise effects for $\kappa/\kappa_d < 1$.

value of $\langle k \rangle$ obtained from standard HIT DNS (run 0), seems to be relatively larger. However, it should be recalled how the accurate convergence of this statistics, which belongs to large scales, requires averaging over many turnover times. Indeed, the observed $\Delta \langle k \rangle$'s are of the same order of $\langle k \rangle$ fluctuations in standard HIT DNS, under the feedback action of the energy-driving forcing scheme with an averaging time of $T_{av}(P\kappa_f^2)^{1/3} \approx 250$, to which standard HIT averaged values are referred.

The convergence of the measured $\mathcal{G}(\kappa, \tau)$ with respect to the averaging time T_{av} is also verified. In Fig. 4 responses measured with increasingly larger values of T_{av} are shown for run 2 at $Re_\lambda = 94$. Adequate convergence is obtained at representative wave numbers $\kappa/\kappa_d = 0.75$ when $T_{av}/(N_c \Delta \tau) > 920$. At larger averaging times, the response curves become indistinguishable. A similar behavior has been verified for the other numerical experiments reported in Table II.

B. Response function and its scaling in the viscous universal subrange

The response function measured via the procedure illustrated above is first compared with its available analytical

TABLE III. Effect of the white-noise forcing on $\langle \varepsilon \rangle$ and $\langle k \rangle$, for various spatial resolutions. The reference simulations without white noise are indicated as "run 0."

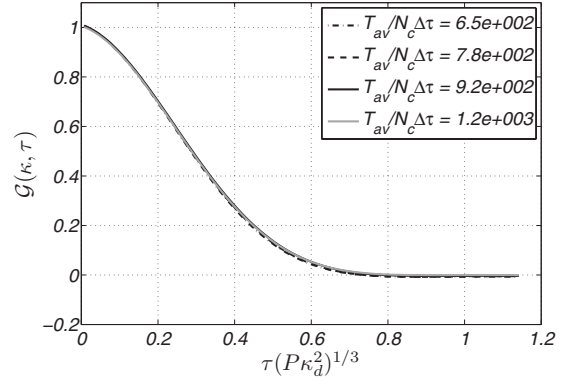| N	Re_λ	Run	$\langle \varepsilon \rangle / P$	$\langle k \rangle / (P/\kappa_f)^{2/3}$	$\Delta \langle \varepsilon \rangle \%$	$\Delta \langle k \rangle \%$
128	55	0	0.999595	4.7856	0.0405	
		1	1.00057	4.7904	0.057	0.1
		2	1.00056	4.7374	0.056	1.007
192	77	0	0.999788	5.0538	0.0212	
		1	1.00177	4.9612	0.177	1.83
		2	1.0025	5.0063	0.25	0.94
256	94	0	1.00155	5.1958	0.155	
		1	1.00268	5.1235	0.113	1.392
		2	1.0007	5.1082	0.085	1.686
		3	1.00354	5.2561	0.354	1.161

FIG. 4. Convergence of the measured $\mathcal{G}(\kappa, \tau)$ with respect to the averaging time T_{av}. Results for run 2 at $Re_\lambda = 94$ (cf. Table II) are shown at representative wave numbers $\kappa/\kappa_d = 0.75$.

approximations, as given in the original DIA theory (see Ref. [1]):

$$\mathcal{G}(\kappa, \tau) = \exp(-\nu \kappa^2 \tau) \frac{J_1(2u_0 \kappa \tau)}{u_0 \kappa \tau}, \qquad (21)$$

and in the analysis of random convection effects [9,21] from which the viscous Gaussian-convective response $\mathcal{G}_{GC}(\kappa, \tau)$ can be introduced:

$$\mathcal{G}_{GC}(\kappa, \tau) = \exp\left(-\nu \kappa^2 \tau - \frac{1}{2} u_0^2 \kappa^2 \tau^2\right), \quad \text{with } \tau > 0. \quad (22)$$

In both previous equations u_0 represents the rms value of turbulent fluctuations, and it can be easily recognized as the Stokes term [Eq. (20)], which reflects the viscous response of the corresponding linear operator. It is important to recall that while the nonviscous term of Eq. (21) is derived as an approximated solution to the DIA equations, the corresponding one of Eq. (22) empirically follows from the analogy with the solution of the idealized problem of *pure random convection* introduced by Kraichnan in Ref. [21] with the random Galilean invariance (RGI) postulate to explain the failure of DIA in yielding a Kolmogorov inertial-range scaling. References [22,23] give a more recent investigation on the role of random convection effects and RGI in renormalized perturbation expansions of the NSEs.

A comparative view of these three response functions at $\kappa/\kappa_d = 1$ is provided in Fig. 5 for $Re_\lambda = 94$, run 3. At time separations smaller than the local energy time scale, i.e., for $\tau u_0 \kappa < 1$, the true measured response is in good agreement with the DIA response function and the viscous Gaussian-convective solution. The latter result does not come as a surprise: even though the turbulent field is definitely non-Gaussian, at times smaller than the characteristic correlation time the Gaussian approximation still applies (see [20]). The unexpected result, however, is that the Gaussian convective solution still approximates very well the measured response at larger times, whereas the DIA solution clearly deviates from it.

This evidence provides further motivation for investigating the convective response scaling in the viscous universal subrange. Response functions rescaled accordingly are plotted in Fig. 6. For the entire range of values of Re_λ considered
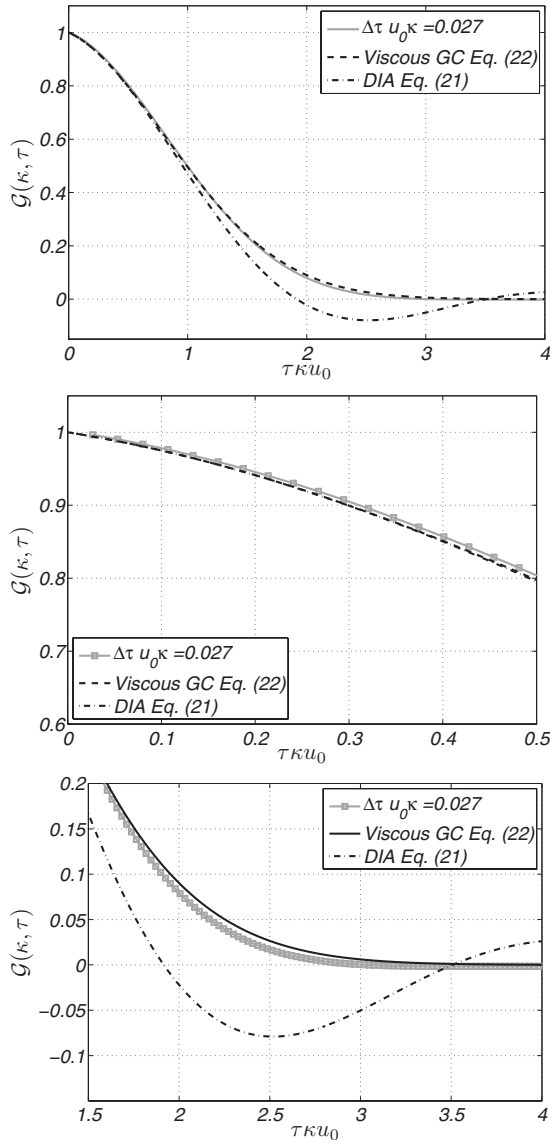
FIG. 6. Measured response functions plotted with convective scaling at different values of Re_λ. The responses are plotted versus nondimensional time separation $\tau u_0 \kappa$, at several wave numbers within the universal dissipative subrange (cf. Table II). Top: $\mathrm{Re}_\lambda = 77$. Bottom: $\mathrm{Re}_\lambda = 94$. For better clarity response functions are plotted using one of every two of the N_c values. Convective scaling produces a good collapse of the curves.

$$\mathcal{Q}_{ij}(\boldsymbol{\kappa}, t, t') = P_{ij}(\boldsymbol{\kappa})\mathcal{Q}(\kappa, t - t'). \tag{24}$$

The correlation function $\mathcal{Q}(\kappa, \tau)$ has been computed thanks to the DNS simulations carried out without white-noise forc-

FIG. 5. Measured response function from run 3 of Table II at $\mathrm{Re}_\lambda = 94$. Top: time decay of the response function at the Kolmogorov scale ($\kappa / \kappa_d = 1$), compared with the DIA solution (21) and the viscous Gaussian-convective solution (22). Center: zoom of the top plot for $\tau \kappa u_0 \ll 1$. Bottom: zoom of the top plot at large $\tau \kappa u_0$.

in the present work, the convective scaling of the response function is clearly assessed. To further support this statement, Fig. 7 shows the response functions tentatively plotted with Kolmogorov viscous scaling: it is evident that such scaling does not produce a good collapse of the different curves when compared to the convective scaling employed in Fig. 6.

C. Correlation function and the FDR

The mean correlation tensor is introduced here directly in its spectral form:

$$\mathcal{Q}_{ij}(\boldsymbol{\kappa}, t, t') = \langle u_i(\boldsymbol{\kappa}, t)u_j(-\boldsymbol{\kappa}, t')\rangle, \tag{23}$$

which reduces to the scalar function $\mathcal{Q}(\kappa, \tau)$ in the homogeneous isotropic stationary case:

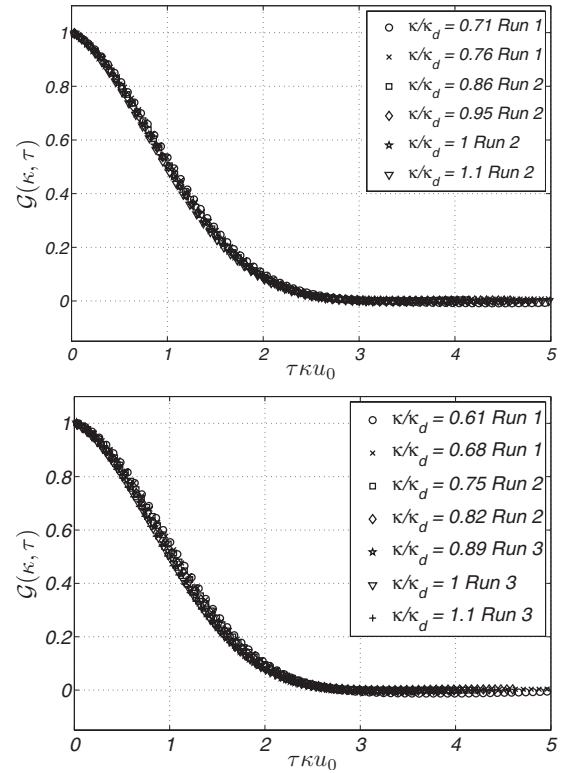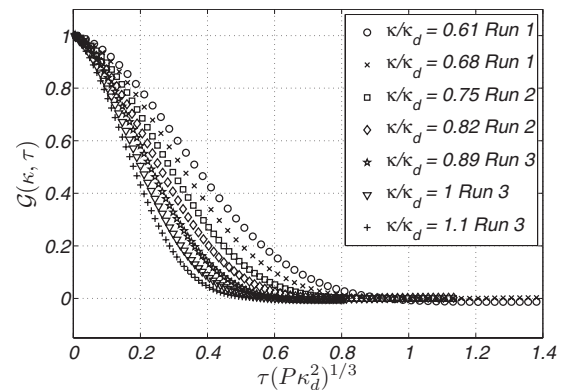
FIG. 7. Measured response functions with Kolmogorov scaling at $\mathrm{Re}_\lambda = 94$. The responses are plotted versus the nondimensional time separation $\tau(P\kappa_d^2)^{1/3}$, at several wave numbers within the universal dissipative subrange (cf. Table II). For better clarity response functions are plotted using one of every two of the N_c values. Kolmogorov scaling is not successful in producing a collapse of the curves.
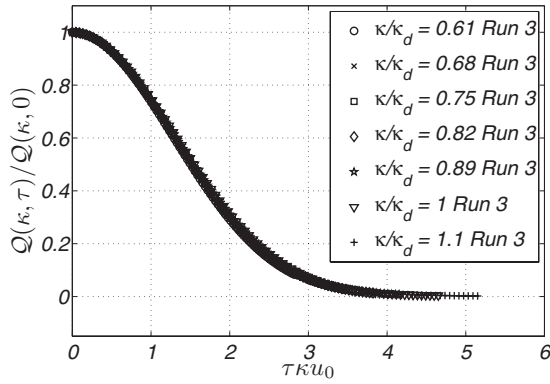
FIG. 8. Measured correlation function plotted with convective scaling. The normalized correlation function is plotted versus nondimensional time separation $\tau u_0 \kappa$, for several wave numbers in the universal dissipative subrange at $Re_\lambda = 94$. Convective scaling produces a good collapse of the curves.

ing. At the various values of Re_λ considered, the corresponding smallest $\Delta\tau$ time resolution employed for measuring the response function has been used. Discretization details can be found in Table II. The number of time separations at which the correlations are stored is $N_c = 200$ for the two cases, respectively, at $Re_\lambda = 55$ and $Re_\lambda = 77$, while $N_c = 175$ has been employed for the case at $Re_\lambda = 94$ due to memory limitations. Proper convergence of the results with respect to T_{av} has been verified, according to what has been done for the response function itself. Similarly to what has been observed for $\mathcal{G}(\kappa, \tau)$, the scaling of the normalized correlation function, $\mathcal{Q}(\kappa, \tau)/\mathcal{Q}(\kappa, 0)$, is captured by the local convective time scale $(\kappa u_0)^{-1}$ in the universal viscous subrange investigated here. This is illustrated for $Re_\lambda = 94$ in Fig. 8, whereas the inadequacy of Kolmogorov viscous scaling is shown in Fig. 9. The same behavior can be also observed to hold for the correlations obtained at $Re_\lambda = 55$ and $Re_\lambda = 77$ (not shown here). The response and correlation functions, as measured from our DNS experiments, can be compared through the well-known FDR

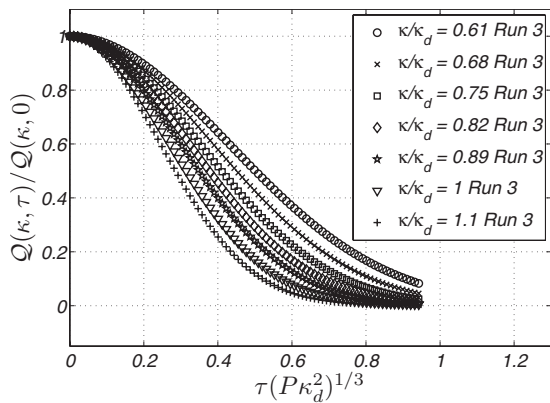$$\mathcal{Q}(\kappa, \tau) = \mathcal{G}(\kappa, \tau)\mathcal{Q}(\kappa, 0). \tag{25}$$

FIG. 9. Measured correlation function plotted with viscous scaling. The normalized correlation function is plotted versus nondimensional time separation $\tau(P\kappa_d^2)^{1/3}$, for several wave numbers in the universal dissipative subrange at $Re_\lambda = 94$. Viscous scaling does not produce a collapse of the curves.

This relation has been originally derived in the context of Hamiltonian dynamical systems at equilibrium for which a canonical distribution holds. Only in the last decades the applicability of the FDR to the wider class of nonlinear chaotic dynamical systems has been addressed on a theoretical basis [24–26]. For this class of systems (to which fluid turbulence belongs) a generalized FDR is demonstrated to hold, provided the system is *dynamically mixing*: only when a Gaussian distribution holds for the invariant probability distribution the generalized FDR reduces to the classical form of Eq. (25). Obviously Eq. (25) cannot be exact for fully developed fluid turbulence, for which both experimental and numerical investigations have shown marked departures from Gaussianity, with long tails in the probability density function and intermittent behavior. However, on an intuitive ground, one would expect a proportionality between the response and the correlation function to hold, at least in terms of characteristic time scales, respectively, indicated by $\tau_{\mathcal{G}}(\kappa)$ and $\tau_{\mathcal{Q}}(\kappa)$ [27]. FDR has been then successfully applied in the context of climate study on sensitivity analysis with respect to external perturbations and parameters [28,29], as well as in viscosity renormalization [30]. Nevertheless, in Refs. [26,29] it is noted how in many such attempts the Gaussian form of the FDR has been often not critically invoked, with little awareness about its inherent limitations. Moreover, in the field of spectral closures, different opinions exist on the possibility to recover the classical FDR in the Eulerian rather than in the Lagrangian framework. In Ref. [5] the Gaussian form of the FDR is exactly recovered within the Lagrangian renormalized approximation of turbulence, where the Lagrangian response function is introduced. In the Eulerian frame the proper use of the FDR has been recently addressed by Kiyani and McComb [7]. In their paper they showed that FDR as stated in Eq. (25) is exact up to second order in renormalized perturbation expansions of NSEs; hence, it can be properly used in related closure formulations [31]. However, Kraichnan suggested [32] that even a valid Gaussian FDR would not immediately be a step forward in the closure problem. In Kraichnan's view, the strong departure from equipartition in the inertial range is not followed by a corresponding strong violation of the Gaussian FDR in the Eulerian frame. This is because large-scale random convection dominates the decay of both the response and the correlation functions, with corresponding time scales for mode κ ruled by the local characteristic convective time $(\kappa u_0)^{-1}$. Kraichnan's analysis thus implies that the local dynamics cannot be captured by the elementary FDR, and the expected deviations can be found only by looking to a generalized FDR that involves a Lagrangian form of the statistics.

These considerations motivate investigating the approximation introduced by the Gaussian FDR within the Eulerian frame: a preliminary assessment is given Fig. 10 where $\mathcal{G}(\kappa, \tau)$ and $\mathcal{Q}(\kappa, \tau)/\mathcal{Q}(\kappa, 0)$ are plotted together for κ fixed at the Kolmogorov scale, i.e., for $\kappa/\kappa_d = 1$. As expected from theoretical arguments (see, for example, Ref. [20]), a longer decorrelation time is observed for $\mathcal{Q}(\kappa, \tau)/\mathcal{Q}(\kappa, 0)$ when compared to $\mathcal{G}(\kappa, \tau)$. However, the time scales $\tau_{\mathcal{G}}(\kappa)$ and $\tau_{\mathcal{Q}}(\kappa)$ turn out to be of the same order. At fixed Re_λ, the plots in convective units of Fig. 10 (top and center) suggest that
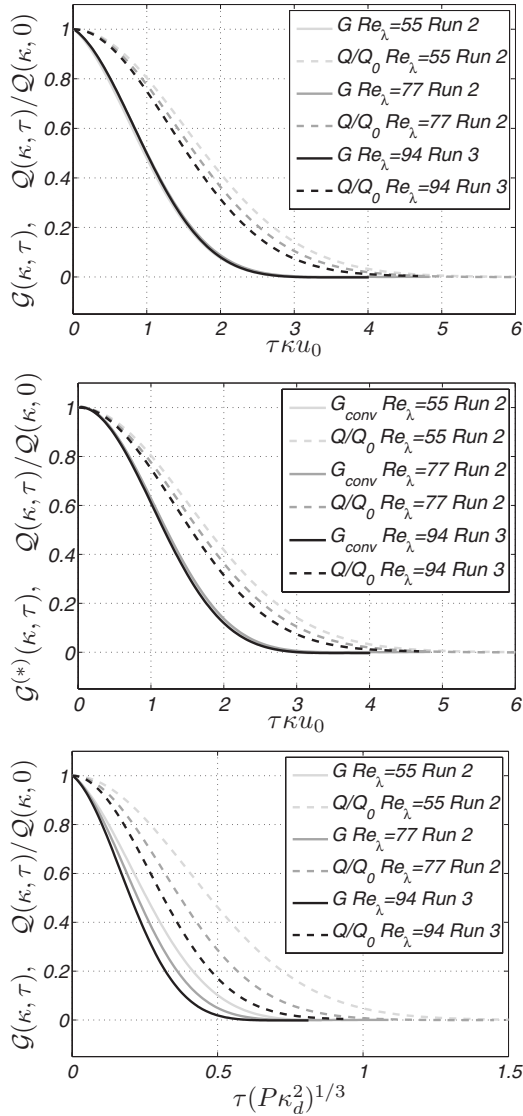
FIG. 10. Measured response functions $\mathcal{G}(\kappa,\tau)$ (continuous lines) and measured normalized correlation functions $\mathcal{Q}(\kappa,\tau)/\mathcal{Q}(\kappa,0)$ (dashed lines) at the Kolmogorov scale $\kappa=\kappa_d$ for several values of Re_λ. Top: convective scaling. Center: convective scaling, but using only turbulent-diffusive part of the response; here $\mathcal{G}^{(*)}(\kappa,\tau) = \mathcal{G}\exp(\nu\kappa^2\tau)$. Bottom: viscous Kolmogorov scaling.

the response and the correlation functions are strictly related within the whole dissipative subrange of scales, owing to their inherent energy-convective scaling property previously discussed.

When examining the response and the correlation functions obtained at different values of Re_λ, one first observes that, in agreement with the very good approximation provided by the analytical viscous Gaussian-convective formulas of Eq. (22) to the response function, the latter is well described as a universal function of the adimensional variable $\tau\kappa u_0$. The same observation does not hold true for the normalized correlation function $\mathcal{Q}(\kappa,\tau)/\mathcal{Q}(\kappa,0)$ which once plotted in convective scaling shows a residual dependence on Re_λ. In particular when increasing Re_λ, the correlation function moves toward the response function, and this implies that the approximation involved by the classical FDR [Eq.

(25)] is gradually improving. For completeness the two functions $\mathcal{G}(\kappa,\tau)$ and $\mathcal{Q}(\kappa,\tau)/\mathcal{Q}(\kappa,0)$ are also plotted in terms of Kolmogorov viscous units, as shown in Fig. 10 (bottom). When this scaling is employed, neither the response nor the correlation shows a collapse.

IV. CONCLUSIONS

The mean linear-response function of homogeneous isotropic turbulence to an impulsive body force has been measured through a number of numerical experiments carried out with DNS, at low and moderate values of the Reynolds number Re_λ. The measurement method leverages a white-noise forcing to probe the flow within the linearity constraint while maintaining the computational effort at reasonable levels. The method employed for measuring the response of the full turbulent flow has been thoroughly validated by computing the response function for purely viscous dynamics: the very same procedure yields this simpler response, for which an exact analytical expression is available to compare with. Based on this test case, the proper convergence with respect to the parameters of the time discretization has been verified. The methodology proposed here for measuring the response function has then proved effective in the quantitative description of the whole time decay of the response within the universal equilibrium range of scales. Our results have been verified both in terms of linearity of the response with respect to the amplitude of the forcing and adequateness of the time averaging. The same direct numerical simulations have been additionally employed for determining the turbulence correlation function. Its examination within the same range of scales has allowed us to preliminarily address the approximations involved by the classical fluctuation- dissipation relation when applied to turbulence dynamics.

The analysis of the response function in the universal dissipative subrange confirms the theoretical prediction of energy-convective scaling for both the response and the normalized correlation functions and, as shown in Figs. 6 and 8, establishes such scaling as the dominant one, at least in the rather limited range of Re_λ considered here. A somewhat surprising result is that the analytical solution provided by Kraichnan in Ref. [21] to the problem of idealized convection turns out to be an extremely good approximation of the measured response function, with small deviations limited to the tail region, as shown in Fig. 5.

When comparing the normalized correlation function and the response function, a longer decorrelation time is observed for the former, as suggested by the theoretical arguments put forward in Ref. [20]. Both $\mathcal{G}(\kappa,\tau)$ and $\mathcal{Q}(\kappa,\tau)/\mathcal{Q}(\kappa,0)$ obey the same convective temporal scaling within the dissipation range; hence, the two time scales $\tau_\mathcal{G}(\kappa)$ and $\tau_\mathcal{Q}(\kappa)$ are in an approximately constant ratio. Obviously the Gaussian form of the FDR [Eq. (25)] is not exactly satisfied, as witnessed from the departure between $\mathcal{G}(\kappa,\tau)$ and $\mathcal{Q}(\kappa,\tau)/\mathcal{Q}(\kappa,0)$ in Fig. 10. Nevertheless, Eq. (25) remains a good approximation in terms of characteristic time scales, even at the moderate value of Re_λ considered here and in the dissipation subrange, where less agreement would be expected in comparison to the inertial subrange, which is the

proper context in which the FDR should be considered [33]. Moreover, the FDR approximation in the present range of scales appears to be increasingly better supported when the value of Re_λ is increased, as shown in Fig. 10. This last conclusion is in partial agreement with a previous study by Biferale *et al.* [12], who examined the response function within the inertial range of scales as extracted from the shell model. In that work the concept of halving-time statistics was introduced to better characterize the time properties of the response function for lower shells, where the proper τ convergence of the response cannot be easily achieved. The ratio between characteristics times is still constant in the inertial range, but $\tau_{\mathcal{Q}}(\kappa)$ and $\tau_{\mathcal{G}}(\kappa)$ show Kolmogorov inertial time scaling. Both Kraichnan's arguments on random convections effects as well as the more recent and related discussion on the validity of the FDR in the context of turbulence [32] are strongly supported by the present results. However, Kraichnan indicated that the dominance of energy-advection effects on both the Eulerian response and the correlation functions is expected to extend to the dissipation range only at high values of Reynolds number, while this has been found in the present work to happen already at low or moderate values of Re_λ addressed here. One possible explanation might be provided by considering the energy-convection effects as a feature of turbulence that remains limited to the dissipative subrange of scales, so that the presence of significant scale separation from the energy scales would let the random convection picture to hold; however, the same could not be true for inertial scales at higher Re_λ.

A more thorough description of the response function and of its relevant time scales, together with a precise assessment of the approximations involved by the classical FDR, obviously calls for an extension of the present study toward much higher values of Re_λ, so that a well-defined inertial range can develop. When such data will be available, the question about a possible asymptotic vanishing of the convective scaling in favor of a true Kolmogorov scaling could be properly answered, thus enlightening the framework of Eulerian closure theories. To this purpose, an analysis using halving-time statistics can be exploited to accurately characterize the properties of the response function in time over a wide range of scales. If Kolmogorov scaling will indeed be recovered at higher Re_λ, then the local relaxation processes of the turbulent response would be captured, opening a new scenario in the understanding of turbulence physics and modeling.

[1] R. H. Kraichnan, J. Fluid Mech. **5**, 497 (1959).

[2] W. McComb J. Phys. A **7**, 632 (1974).

[3] R. H. Kraichnan, Phys. Fluids **8**, 575 (1965).

[4] R. H. Kraichnan, J. Fluid Mech. **83**, 349 (1977).

[5] Y. Kaneda, J. Fluid Mech. **107**, 131 (1981).

[6] S. Kida and S. Goto, J. Fluid Mech. **345**, 307 (1997).

[7] K. Kiyani and W. McComb, Phys. Rev. E **70**, 066303 (2004).

[8] T. Ishihara, T. Gotoh, and Y. Kaneda, Annu. Rev. Fluid Mech. **41**, 165 (2009).

[9] W. McComb, *The Physics of Fluid Turbulence* (Oxford University Press, New York, 1990).

[10] W. McComb, M. J. Filipiak, and V. Shanmugasundaram, J. Fluid Mech. **245**, 279 (1992).

[11] Y. Kaneda, Phys. Fluids **5**, 2835 (1993).

[12] L. Biferale, I. Daumont, G. Lacorata, and A. Vulpiani, Phys. Rev. E **65**, 016302 (2001).

[13] P. Luchini, M. Quadrio, and S. Zuccher, Phys. Fluids **18**, 121702 (2006).

[14] P. Sagaut and C. Cambon, *Homogeneous Turbulence Dynamics* (Cambridge University Press, Cambridge, England, 2008).

[15] C. Canuto, M. Y. Hussaini, A. Quarteroni, and T. A. Zang, *Spectral Methods—Fundamentals in Single Domains* (Springer, New York, 2006).

[16] C. Canuto, M. Y. Hussaini, A. Quarteroni, and T. A. Zang, *Spectral Methods: Evolution to Complex Geometries and Applications to Fluid Dynamics* (Springer, New York, 2007).

[17] A. G. Lamorgese, D. A. Caughey, and S. B. Pope, Phys. Fluids **17**, 015106 (2005).

[18] A. H. Jazwinski, *Stochastic Processes and Filtering Theory* (Academic Press, New York, 1970).

[19] Note that a white-noise field with identity covariance matrix is used in the definition of $\delta f_j(\boldsymbol{\kappa},t)$ [Eq. (13)]: the identity covariance scaling factor for $w_j(\boldsymbol{\kappa},t)$ could be easily embedded in the definition of ϵ without losing of generality.

[20] D. C. Leslie, *Developments in the Theory of Turbulence* (Clarendon Press, Oxford, 1973).

[21] R. H. Kraichnan, Phys. Fluids **7**, 1723 (1964).

[22] W. McComb, V. Shanmugasundaram, and P. Hutchinson, J. Fluid Mech. **208**, 91 (1989).

[23] W. McComb, Phys. Rev. E **71**, 037301 (2005).

[24] M. Falcioni, S. Isola, and A. Vulpiani, Phys. Lett. A **144**, 341 (1990).

[25] G. F. Carnevale, M. Falcioni, S. Isola, R. Purini, and A. Vulpiani, Phys. Fluids A **3**, 2247 (1991).

[26] U. Marconi, A. Puglisi, L. Rondoni, and A. Vulpiani, Phys. Rep. **461**, 111 (2008).

[27] $\tau_{\mathcal{G}}(\kappa)$ and $\tau_{\mathcal{Q}}(\kappa)$ are to be intended, respectively, as the separation time τ by which $\mathcal{G}(\kappa,\tau)$ and $\mathcal{Q}(\kappa,\tau)$ reduce to the same percentage of their initial value.

[28] T. L. Bell, J. Atmos. Sci. **37**, 1700 (1980).

[29] G. Lacorata and A. Vulpiani, Nonlinear Processes Geophys. **14**, 681 (2007).

[30] G. F. Carnevale and J. S. Frederiksen, J. Fluid Mech. **131**, 289 (1983).

[31] W. McComb and K. Kiyani, Phys. Rev. E **72**, 016309 (2005).

[32] R. H. Kraichnan, Physica A **279**, 30 (2000).

[33] *Statistical Models and Turbulence*, edited by M. Rosenblatt and C. Van Atta (Springer-Verlag, Berlin, 1972), Vol. 12, pp. 148–194.